https://doi.org/10.5194/egusphere-2023-2186
Preprint. Discussion started: 11 October 2023

Spring tropical cyclones modulate near-surface isotopic compositions of atmospheric water vapour at Kathmandu, Nepal

Niranjan Adhikari[1, 2], Jing Gao[1, 3,*], Aibin Zhao[1], Tianli Xu[1, 4] Manli Chen[1, 3], Xiaowei Niu[1], Tandong Yao[1, 3]

[1] *State Key Laboratory of Tibetan Plateau Earth System, Resources and Environment, Institute of Tibetan Plateau Research, Chinese Academy of Sciences, Beijing 100101, China*

[2] *University of Chinese Academy of Sciences, Beijing 100049, China*

[3] *Lanzhou University, Lanzhou 733000, China*

[4] *Kathmandu Centre for Research and Education*, Chinese Academy of Sciences –*Tribhuvan University, Kirtipur 44613, Kathmandu, Nepal*

* Correspondence to: Jing Gao, E-mail: gaojing@itpcas.ac.cn

Abstract

The Arabian Sea (AS) and the Bay of Bengal (BoB) are the major part of the Indian Ocean where cyclonic activities prevail each year, resulting in extreme precipitation events, particularly during the pre-monsoon season. Despite the significance of cyclones in Nepal, no studies have investigated their impact on the isotopic composition of atmospheric water vapour ($\delta^{18}O_v$, δD_v, and d-excess$_v$). Here, we present the results of continuous measurements of the isotopic composition of atmospheric water vapour at Kathmandu from 7 May to 7 June 2021 during two pre-monsoon cyclone events, namely cyclone Tauktae formed over the Arabian Sea, and cyclone Yaas formed over the Bay of Bengal. We observed a significant depletion of $\delta^{18}O_v$ and δD_v during both cyclone events compared to before and after the cyclone events which was

https://doi.org/10.5194/egusphere-2023-2186
Preprint. Discussion started: 11 October 2023

attributed to changes in moisture sources (local vs. marine) as inferred from backward moisture trajectories. The outgoing longwave radiation (OLR) and regional precipitation during cyclone events together with the observed correlation between vertical velocity and $\delta^{18}O_v$ showed high moisture convergence and heavy convection at and around the measurement site which caused unusually depleted $\delta^{18}O_v$ during that period. Moisture convergence and convection were stronger during cyclone Yaas which resulted in higher (lower) d-excess$_v$ ($\delta^{18}O_v$), compared to Tauktae, possibly due to strong downdrafts during the cyclone-related rain events which can transport vapour with higher (lower) d-excess$_v$ ($\delta^{18}O_v$) toward the surface. Our study reveals that tropical cyclones that originated from the BoB and the AS modulate isotopic signals of near-surface atmospheric water vapour considerably in Nepal. Hence caution should be made while interpreting the isotopic variability during the non-monsoon season and the effect of cyclones on the isotopic composition of precipitation and atmospheric water vapour. Our results shed light on key processes governing the isotopic composition of atmospheric water vapour at Kathmandu and may have implications for the paleoclimate reconstruction of tropical cyclone activity.

Keywords: Cyclones; Bay of Bengal; Arabian Sea; Isotopic composition of atmospheric water vapour; Convection; Moisture convergence; Kathmandu

https://doi.org/10.5194/egusphere-2023-2186
Preprint. Discussion started: 11 October 2023

1 Introduction

Although the Indian summer monsoon accounts for more than 80 % of annual rainfall in Nepal, agricultural activities also crucially rely on precipitation in the spring season (also known as the pre-monsoon season). Pre-monsoonal rainfall in Nepal is often associated with cyclonic events that provide sufficient moisture for precipitation to support the timely planting of monsoonal crops. Every year, cyclonic events over the North Indian Ocean result in extreme precipitation events, particularly during the pre-monsoon season with less extreme events during the post-monsoon season (Li et al., 2013). Previous studies have suggested that extreme precipitation in Nepal is mostly fuelled by moisture from the Arabian Sea (AS) and the Bay of Bengal (BoB) (Bohlinger et al., 2017; Boschi and Lucarini, 2019). High sea surface temperatures and the westward movement of tropical cyclones formed over the Western Pacific result in cyclones being formed over the BoB and AS (Mohapatra et al., 2016). The number of cyclones in the AS has dramatically increased in recent years compared to the number of cyclones in the BoB (Pandya et al., 2021). According to the International Best Track Archive for Climate Stewardship (IBTrACS) project, in 2019 three cyclones originated in the BoB while five cyclones originated in the AS. This increase in cyclone frequency in the AS may be due to a rise in sea surface temperature which also lengthens the cyclone decay period (Li and Chakraborty, 2020). Usually, the impact of cyclones formed over the AS is restricted to the nearest coastal regions. However, in recent years this appears to have changed as cyclones are forming back-to-back over the AS and affecting the entire Indian subcontinent including surrounding regions, likely due to AS warming leading to cyclone intensification (Li and Chakraborty, 2020). Cyclone Tauktae has affected the livelihoods of people both near the coast and further inland during the pre-monsoon season of 2021 (Pandya et al., 2021). The impacts of cyclone Yaas after cyclone

https://doi.org/10.5194/egusphere-2023-2186
Preprint. Discussion started: 11 October 2023

Tauktae were also felt in Nepal, where it triggered flooding and landslides in several parts of the country **(**https://floodlist.com/asia/nepal-flood-landslide-may-2021/**).** As both cyclones hit in short succession, this led to severe agricultural damage in several parts of India at a critical time when farmers were preparing to sow their rice paddies ahead of the monsoon season (https://reliefweb.int/organization/acaps). In Nepal, most of the damage due to Yaas was mostly limited to the Terai regions which experienced intense and continuous rainfall **(**https://kathmandupost.com/). At the same time, some hilly regions benefited from these cyclone-induced rains, as they created favourable conditions for farmers preparing their monsoonal crops. Moisture flux associated with cyclones generally extends over a large area and causes moderate to heavy precipitation along the cyclone path and on the nearest land mass (Chan et al., 2022; Rajeev and Mishra, 2022). Thus, it is essential to understand the influence of these extreme rainfall events on atmospheric water vapour, which are in turn related to local clouds and surface energy budgets, determining the amount of moisture available to plants.

Atmospheric water vapour is an important constituent of the hydrological cycle and climate system (Saranya et al., 2017), mainly because of its impacts on solar radiation absorption, cloud formation, and atmospheric heating (Noone, 2012). With global warming, the amount of water vapour in the atmosphere is also expected to increase. This has created scientific interest in a variety of fields to elucidate the impact of atmospheric water vapour on changing moisture patterns (Hoffmann et al., 2005).

The isotopic composition of atmospheric water vapour ($\delta^{18}O_v$, $\delta D_{v,}$ and d-excess$_v$) contains comprehensive information about the hydrological cycle and the history of moisture exchange (Noone, 2012; Payne et al., 2007; Risi et al., 2008; Worden et al., 2007). Several studies have shown that the isotopic composition of atmospheric water vapour is an effective

https://doi.org/10.5194/egusphere-2023-2186
Preprint. Discussion started: 11 October 2023

indicator of cyclone activity (Munksgaard et al., 2015; Sun et al., 2022) including cyclone evolution and structure (Lawrence et al., 2002). The atmospheric water vapour and precipitation associated with tropical cyclones tend to have extremely depleted isotopic compositions compared to monsoonal rain (Chen et al., 2021; Jackisch et al., 2022; Munksgaard et al., 2015; Sánchez-Murillo et al., 2019), which may be due to the high condensation efficiency and substantial fractionation associated with cyclones. A few studies found a systematic depletion of heavy isotopes towards the cyclone eye (Lawrence et al., 2002, 1998; Lawrence and Gedzelman, 1996; Sun et al., 2022; Xu et al., 2019). For instance, studying the cyclone Shanshan on Ishigaki Island, southwest of Japan, Fudeyasu (2008) observed that isotopic depletion in precipitation and water vapour increased radially inward in the cyclone's outer region, likely due to a rainout effect associated with condensation efficiency and the isotopic exchange between precipitation and water vapour. A study conducted in north-eastern Australia during cyclone Ita in April 2014 highlighted the role of synoptic-scale meteorological settings in determining the isotopic variability of atmospheric water vapour (Munksgaard et al., 2015). In Fuzhou, China, Xu et al., (2019) reported a significant depletion in typhoon rain $\delta^{18}O$ which was related to the combined effect of large-scale convection, high condensation efficiency, and recycling of isotopically depleted vapour in the rain shield area. Sánchez-Murillo et al., (2019) highlighted the role of convective and stratiform activity as well as precipitation type and amount as the main controlling factors of precipitation stable isotopes associated with tropical cyclones. The impact of high stratiform fractions and deep convection on isotopic depletion in precipitation during typhoon Lekima was confirmed by Han et al., (2021). These findings clearly demonstrate that the processes that contribute to high-frequency shifts in the isotopic composition of precipitation and atmospheric water vapour during tropical cyclones are still a matter of debate.

Although several studies have examined the isotopic variation of event-based precipitation in Nepal (Acharya et al., 2020; Adhikari et al., 2020; Chhetri et al., 2014), there remains a knowledge gap regarding the isotopic response of atmospheric water vapour during cyclone events. Here, we present for the first time the evolution of the isotopic composition of atmospheric water vapour ($\delta^{18}O_v$, δD_v, and d-excess) in Kathmandu during two pre-monsoon cyclone events. Isotopic data were provided in 2021, stretching from one week before to one week after the cyclone events. Although neither cyclone passed directly over Kathmandu, their remnant vapour produced several days of rainfall over Kathmandu which enabled us to observe changes in the isotopic composition of atmospheric water vapour at high temporal resolutions and to evaluate the cause of such changes at daily and diurnal scales.

2 Data and methods

2.1 Site description

The Kathmandu station lies on the southern slope of the Himalayas (27°42′ N, 85°20′ E) at an average altitude of about 1400 m above sea level. Based on an 18-year-long record (from 2001 to 2018) (Figure 1), this region has an average annual temperature of about 19° C and average annual precipitation of 1500 mm, with most of the rainfall occurring in the monsoon season (June to September) (Adhikari et al., 2020). About 16 % of total annual rainfall in Kathmandu occurs in the pre-monsoon season (March to May) with a corresponding mean maximum (minimum) air temperature of 28° C (13° C) and relative humidity (RH) of 67 %. The total moisture flux (sum of zonal and meridional fluxes) during the pre-monsoon season is low (<60 kg/m/s) as is specific humidity (~6 g/kg), which is associated with transport by westerlies. The region receives about 78 % of its annual rainfall during the monsoon season with associated

https://doi.org/10.5194/egusphere-2023-2186
Preprint. Discussion started: 11 October 2023

mean maximum (minimum) air temperature of 29° C (20° C) and RH of about 82 %. Most of the precipitation over Kathmandu during the monsoon period is due to the influx of humid air masses from the BoB. Average post-monsoon (October and November) and winter (December to February) RH is about 80 % and 78 %, respectively, with similar rainfall contributions (3 %) during both seasons. The mean post-monsoon and winter mean maximum (minimum) air temperature is about 25° C (11° C) and 21° C (4° C), respectively.

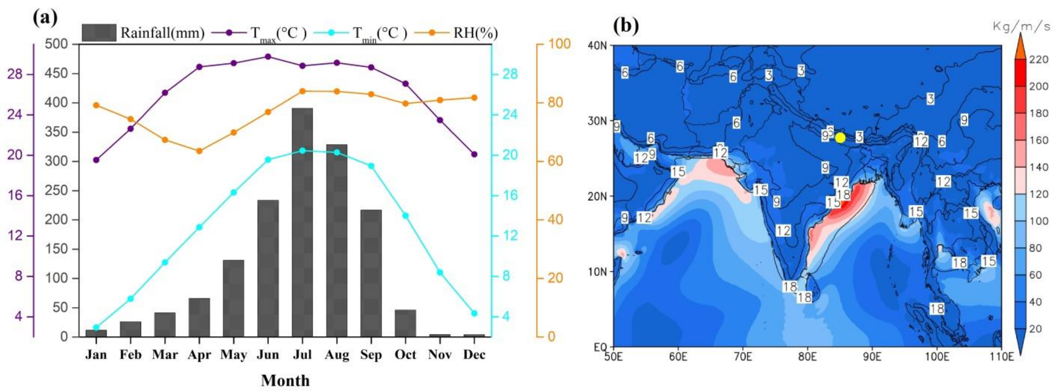

Figure 1 (a) Long-term (2001-2018) average monthly maximum temperatures (T_{max}), minimum temperature (T_{min}), relative humidity (RH), and precipitation amount (P) at Kathmandu. (b) Spatial distribution of long-term (1990-2021) average specific humidity (in g/Kg) (contour lines) and mean vertically integrated moisture flux (colour) during the pre-monsoon season. The yellow dot shows the location of the Kathmandu site.

2.2 The evolution of cyclones Tauktae and Yaas

Cyclone Tauktae developed as a tropical disturbance on 13 May 2021 over the AS and had evolved into a deep depression by 14 May, moving northward and gradually intensifying over the warm coastal water before turning into a cyclonic storm with wind speeds reaching 75 km/h on that same day (Pandya et al., 2021). Even after making landfall in the Gir-Somnath district of

Gujarat, Tauktae continued to strengthen and was classified as an extremely severe cyclonic storm on 17 May reaching maximum wind speeds of 220 km/h as per the Indian Meteorological Department's Tropical Cyclone Intensity Scale (Verma and Gupta, 2021; Pandya et al., 2021). Cyclone weakened into a low depression on 18 May 2021 at 17:00 h Indian Local Time (ILT) and finally dissipated one day later. Due to its large convective area, it brought heavy rainfall to different regions of India and Nepal.

Cyclone Yaas started out as a depression over the BoB on 22 May 2021 at 08:30 h ILT and gradually intensified into a deep depression before turning into a cyclonic storm on 24 May at around 00:00 h ILT as it moved northeast (Paul and Chowdhury, 2021). The corresponding wind speed and central pressure were recorded as about 65 km/h and 990 hPa, respectively. On 24 May at around 18:00 h ILT, it intensified into a severe cyclonic storm with wind speeds ranging from 89 to 117 km/h before becoming a very severe cyclonic storm on 25 May at 12:00 h ILT with wind speeds from about 119 km/h to 165 km/h. It made landfall north of Odisha on 26 May with maximum sustained wind speeds of 130 km/h to 140 km/h and progressively weakened into a depression on 27 May and dissipated over northern India on 28 May.

2.3 Isotope measurements and meteorological data

Near-surface $\delta^{18}O_v$ and δD_v were measured continuously using a Picarro L2130-i analyser based on wavelength-scanned cavity ring-down spectroscopy (WS-CRDS) (Brand et al., 2009), located at the Kathmandu Centre for Research and Education (KCRE), established by the Chinese Academy of Sciences with the collaboration of Tribhuvan University, Nepal. An inlet of water vapour was placed 7 m above the grass-covered ground. The copper tube is heated using a self-regulating heat trace isolated with armaflex. To prevent rain from being sucked into the tube, the head of the inlet was covered with a plastic hood. A 10 L min^{-1} pump quickly transported the

https://doi.org/10.5194/egusphere-2023-2186
Preprint. Discussion started: 11 October 2023

vapour from the inlet to the analyser. The automated standard delivery module (SDM) was used for standard calibration. Each calibration was made with two reference standards that had been calibrated against Vienna Standard Mean Ocean Water (VSMOW) covering the isotopic ranges of ambient water vapour at Kathmandu. Each reference standard was measured continuously for a total of 75 min each day at three different humidity levels (25 min per level). The evaporated standard was then mixed with dry air obtained via Drierite™ desiccant (Merck, Germany) and finally delivered to the Picarro analyser for isotopic measurements. The isotopic composition of atmospheric water vapour is reported as parts per thousand (‰) relative to VSMOW using

$$\boldsymbol{\delta^* = (R_A / R_S - 1) \times 1000\ [‰]}, \quad \textbf{(1)}$$

where δ^* represents either δD_v or $\delta^{18}O_v$, and R_A and R_S denote the ratios of heavy to light isotopes ($^{18}O/^{16}O$ or D/H) in the sample and standard, respectively (Kendall & Caldwell, 1998; Yoshimura, 2015). As suggested by Dansgaard, (1964), deuterium excess (d-excess$_v$= δD_v-8×$\delta^{18}O_v$) is used as a tracer for moisture source conditions (Liu et al., 2008; Tian et al., 2001). We presented hourly isotopic composition of atmospheric water vapour between 7 May and 7 June 2021, covering the Tauktae and Yaas cyclone events (see previous section) including 1 week on either side of the events. An automated weather station (AWS) continuously measured air temperature, relative humidity, dew point temperature, wind speed and direction, rainfall amount, surface pressure, etc. at a sampling rate of 1 min^{-1}.

2.4 Cyclone track data

The International Best Track Archive for Climate Stewardship (IBTrACS) project containing best-track datasets of recent and historical tropical cyclones was used to obtain the cyclone track data for this study (Knapp et al., 2010). We downloaded wind speeds, pressure, and cyclone eye location information (3-hour resolution) from

https://doi.org/10.5194/egusphere-2023-2186
Preprint. Discussion started: 11 October 2023

https://www.ncei.noaa.gov/products/. The latter was used to calculate the spatial distance between the cyclone's eye and our measurement location.

2.5 Satellite precipitation and Outgoing Longwave Radiation data

We used Integrated Multi-satellite Retrievals for GPM (IMERG) from the Global Precipitation Measurement (GPM) program with a spatial resolution of 0.1° latitude and longitude to analyse the regional rainfall intensity before, during, and after the cyclone events, following a previously reported method (Huffman et al., 2017). These high-resolution IMERG data allow for the identification of convective rainfall areas and the passage of tropical cyclones (Jackisch et al., 2022) and have been used previously to depict cyclone tracks and associated rainfall intensities (Gaona et al., 2018; Jackisch et al., 2022; Villarini et al., 2011).

For outgoing longwave radiation (OLR), we used the National Centers for Environmental Prediction (NCEP) daily reanalysis of datasets, with a spatial precision of 2.5° from longitude-latitude grids (available at https://www.esrl.noaa.gov/psd/ (Kleist et al., 2009). OLR data has already been used as an index of tropical convection (Liebmann and Smith, 1996). We further obtained zonal and meridional wind, specific humidity, vertical velocity, vertical pressure, and vertical distribution of relative humidity and temperature data from ERA5 datasets with a spatial resolution of 0.25° from longitude-latitude grids (https://cds.climate.copernicus.eu/).

2.6 Moisture backward trajectory analysis

To assess the influence of moisture transport history on the isotopic composition of atmospheric water vapour before, during, and after the cyclone events, we analysed 5-day moisture backward trajectories that terminated at the sampling site using the Hybrid Single-Particle Lagrangian Integrated Trajectory (HYSPLIT) model (Draxler and Hess, 1997). The

https://doi.org/10.5194/egusphere-2023-2186
Preprint. Discussion started: 11 October 2023

Global Data Assimilation System (GDAS) with a spatial resolution of 1° (Kleist et al., 2009) was used to provide the meteorological forcing for the HYSPLIT model. Variations in specific humidity along the moisture trajectories were also calculated. Since most of the atmospheric vapour is contained within the bottom 2 km, we set the initial starting height for the moisture backward trajectories to 500 m above ground. Additionally, using ERA5 datasets, we determined the average boundary layer height at Kathmandu during the study period as about 620 m, which confirms 500 m as an appropriate choice for the initial starting height to derive the moisture trajectories.

https://doi.org/10.5194/egusphere-2023-2186
Preprint. Discussion started: 11 October 2023

3 Results and discussion

3.1 Water vapour isotope evolution before, during, and after cyclone events

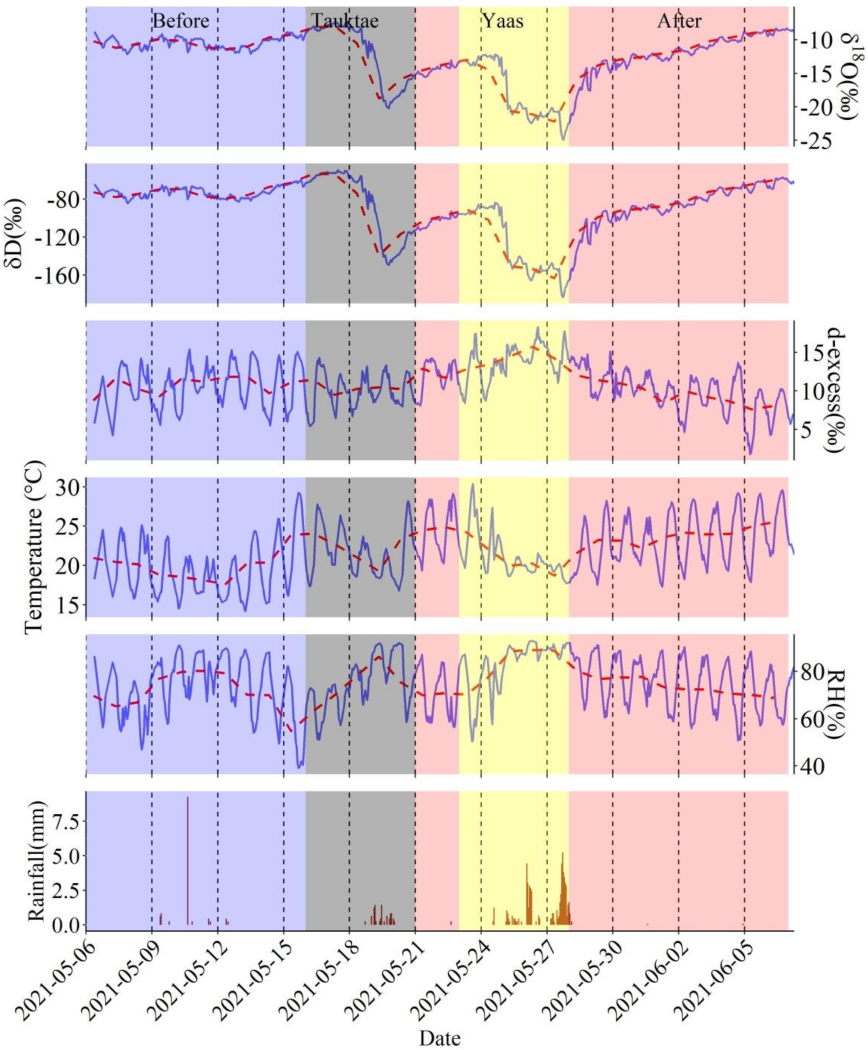

Figure 2 Water vapour isotopic evolution (hourly averages) before, during, and after the Tauktae and Yaas cyclone events along with associated surface air temperature, relative humidity (RH), and rainfall amount. The red dashed line in the figure represents daily variations.

https://doi.org/10.5194/egusphere-2023-2186
Preprint. Discussion started: 11 October 2023

The isotopic composition of atmospheric water vapour surrounding the two cyclone events shows significant variability at Kathmandu station (Figure 2, Table 1). $\delta^{18}O_v$ and δD_v showed a sudden depletion in the final stages of both cyclones, which coincides with RH reaching its maximum values. The depletion was more pronounced during cyclone Yaas compared to cyclone Tauktae. Before the cyclone Tauktae, $\delta^{18}O_v$ (δD_v) varied from -8.38 ‰ (-60.10 ‰) to -12.10 ‰ (-84.15 ‰) with an average of -10.52 ‰ (-73.22 ‰) and d-excess$_v$ ranged from 4.24 ‰ to 15.28 ‰ with an average of 10.94 ‰. The highest $\delta^{18}O_v$ value of -7.40 ‰ was observed before the cyclone Tauktae, whereas the lowest $\delta^{18}O_v$ value of -24.92 ‰ was observed during the final stages of cyclone Yaas. Clearly, the isotopic composition of atmospheric water vapour shows a downward trend as the remnant of cyclones passed over Kathmandu. $\delta^{18}O_v$ decreased by over 12 ‰ from 14 May to 20 May (Tauktae) and again between 24 May and 29 May (Yaas), reaching minima for $\delta^{18}O_v$ (δD_v) of -20.21 ‰ (-149.49 ‰) and -24.92 ‰ (-183.34 ‰), respectively. During Tauktae, d-excess$_v$ varied from 6.47 ‰ to 18.79 ‰ with an average of 10.87 ‰ while during Yaas it varied from 8.71 ‰ to 18.29 ‰ with an average of 13.77 ‰. After both cyclones had dissipated, $\delta^{18}O_v$ (and δD_v) started to recover pre-cyclone values of -8.29 ‰ to -14.94 ‰ (-57.40 ‰ to -109.31 ‰), with an average of -11.09 ‰ (-79.38 ‰). During that period, d-excess ranged between 1.80 ‰ and 15.11 ‰ with an average of 9.37 ‰. Notably, the isotopic composition of atmospheric water vapour before the commencement of rainfall by Tauktae remained enriched, suggesting that the isotopic composition of atmospheric vapour during that period was representative of surface layer inflow (Munksgaard et al., 2015). However, $\delta^{18}O_v$ and δD_v at the earlier stage of cyclone Yaas were significantly lower as compared to the earlier stage of cyclone Tauktae. These discrepancies might be due to the timing of their occurrence or the convective strength. The passage of cyclones that had formed over the

https://doi.org/10.5194/egusphere-2023-2186
Preprint. Discussion started: 11 October 2023

AS (Tauktae) and BoB (Yaas) caused significant depletion in the isotopic composition of atmospheric water vapour and led to cumulative rainfall of 9.2 mm (Tauktae) between 14 May and 20 May 2021 and 59.6 mm (Yaas) between 25 May and 28 May 2021 at our site. This is in agreement with previous studies which documented similar depletion in isotope ratios due to cyclone-associated intense rainfall (Krishnamurthy and Shukla, 2007; Rahul et al., 2016). It is noteworthy that the above $\delta^{18}O_v$ minimum observed during cyclone Yaas is similar to the minimum observed in Bangalore, India ($\delta^{18}O_v$ =-22.5 ‰) (Rahul et al., 2016) and Roorkee, India ($\delta^{18}O_v$ =-25.35 ‰) (Saranya et al., 2018) when cyclones evolved over the BoB, were closest to their sampling sites. These results indicate the significant impact of oceanic moisture on the isotopic composition of atmospheric water vapour over the continental during the time of cyclones. We will discuss the influence of moisture sources in Sect. 3.3 in more detail.

The relation between $\delta^{18}O_v$ and δD_v varies for the periods before, during, and after the cyclones, showing different slopes and intercepts with the Local Meteoric Vapour Line (LMVL) (Figure 3). Before the first cyclone event, both the slope and intercept are significantly lower (slope=5.85 and intercept= -12.12), indicating the strong influence of non-equilibrium processes such as evaporation. During both cyclone events, both the slopes and intercepts resemble the slope and intercept of the global meteoric water line (GMWL: $\delta D=8\times\delta^{18}O+10$) (Figure 3). After the cyclone events, the slope and intercept decreased to 7.37 and to 2.34, respectively, which implies a change of moisture sources and evaporation becoming dominant once again.

https://doi.org/10.5194/egusphere-2023-2186
Preprint. Discussion started: 11 October 2023

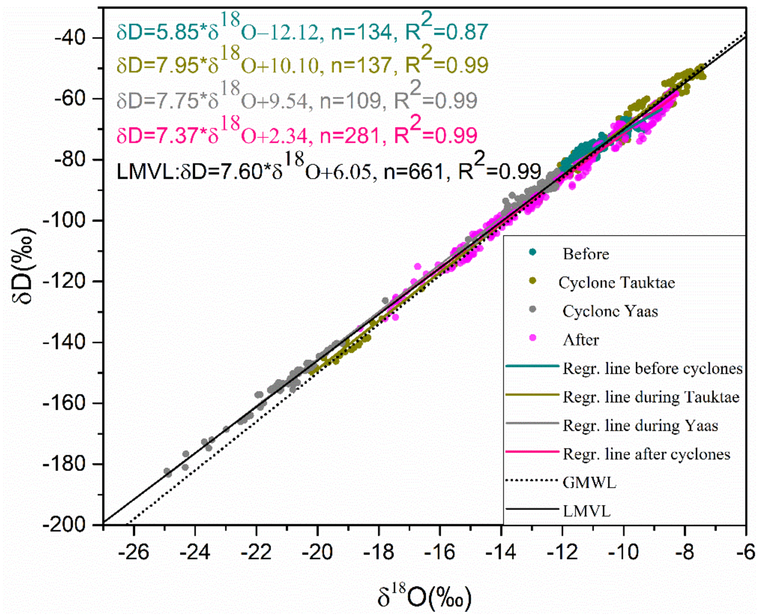

Figure 3 Relationships between $\delta^{18}O_v$ and δD_v before, during, and after the cyclone events. The regression lines for each period are presented along with GMWL for comparison.

Table 1 Descriptive statistics of $\delta^{18}O_v$, δD_v, and d-excess$_v$ measured before, during, and after the cyclone events.

Period	$\delta^{18}O_v$ [‰]			δD_v [‰]			d-excess$_v$ [‰]		
	min	max	avg	min	max	avg	min	max	avg
Before	-12.10	-8.38	-10.52	-84.15	-60.10	-73.22	4.24	15.38	10.94
Cyclone Tauktae	-20.21	-7.40	-13.59	-149.49	-49.53	-97.88	6.47	18.79	10.87
Cyclone Yaas	-24.92	-12.17	-17.87	-183.34	-83.85	-129.18	8.71	18.29	13.77
After	-14.94	-8.29	-11.09	-109.31	-57.40	-79.38	1.80	15.11	9.37

https://doi.org/10.5194/egusphere-2023-2186
Preprint. Discussion started: 11 October 2023

3.2 Day-to-day and diurnal variations during cyclones events

To understand the depletions in $\delta^{18}O_v$ and δD_v during the Tauktae and Yaas cyclone events, we analysed the regional wind fields and specific humidity over the Northern Indian Ocean during the respective periods. Fig. S3 shows the genesis, development, movement, and dissipation of cyclone Tauktae together with changes in specific humidity along the transport path. The remnants of cyclone Tauktae caused light rain at Kathmandu, with a significant depletion in $\delta^{18}O_v$ (δD_v) by ~8 ‰ (~66 ‰) on 20 May as compared to the previous day. From the formation of a depression over the AS on 14 May 2021 until the commencing dissipation inland on 19 May, no significant variation in the isotopic composition of atmospheric water vapour was observed (Fig. 2). After the dissipation, when the residual Tauktae vapour passed the Kathmandu producing light rains, $\delta^{18}O_v$ and δD_v began to decrease independently of the rainfall amount, starting on 19 May at around 11:00 h Local Time (LT) from -8.34 ‰ for $\delta^{18}O_v$ and -56.06 ‰ for δD_v and dropping in just one hour to -10.12 ‰ and -68.41 ‰ respectively. This decrease continued for another day, reaching a minimum of -20.21 ‰ and -149.49 ‰ for $\delta^{18}O_v$ and δD_v respectively on 20 May at around 12:00 h LT. However, d-excess$_v$ did not show notable variations during the passage of cyclone Tauktae. $\delta^{18}O_v$ and δD_v remained anomalously depleted from 20 to 22 May due to the presence of a remnant of cyclone Tauktae.

On 24 May, cyclone Yaas formed over the BoB and started along a northward trajectory through north-eastern India (Fig. S4). The high specific humidity over India and surrounding regions during the days of cyclone formation indicates that Yaas had lifted a large amount of water vapour from the BoB, which subsequently produced intense rainfall along its path. The effect of cyclone Yaas on $\delta^{18}O_v$ and δD_v at Kathmandu was first captured on 25 May with $\delta^{18}O_v$ (δD_v) dropping rapidly from -12.62 ‰ (-88.71 ‰) on 25 May at 20:00 h LT to -15.07 ‰ (-

https://doi.org/10.5194/egusphere-2023-2186
Preprint. Discussion started: 11 October 2023

106.22 ‰) just one hour later. At the same time, d-excess$_v$ was increased from 12.30 ‰ to 14.34 ‰. The depletion continued until 28 May with a minimum of $\delta^{18}O_v$ (δD_v) by -24.92 ‰ (-182.35 ‰) at 16:00 h LT. At that time, Yaas had already weakened into a low-pressure area over Bihar in south-eastern Uttar Pradesh, India. $\delta^{18}O_v$ and δD_v started to increase after Yaas had dissipated, reaching -14.64 ‰ for $\delta^{18}O_v$ and -103.97 ‰ for δD_v on 29 May at 16:00 h LT. From 25 to 29 May, d-excess$_v$ gradually increased, resulting in a strong negative association with $\delta^{18}O_v$ and δD_v, with correlation coefficients of -0.60 and -0.55 respectively. Such strong isotopic depletion during cyclone events might be associated with high condensation efficiencies within the cyclones leading to extensive fractionation (Rahul et al., 2016).

To further elucidate the processes affecting the diurnal variability of the isotopic composition of atmospheric water vapour, we investigated the mean diurnal cycles of $\delta^{18}O_v$, δD_v, d-excess$_v$, surface temperature, and specific humidity during the cyclone events, focussing on the last 4 days of each cyclone (19 May to 22 May for Tauktae and 25 May to 28 May for Yaas) when the measurement site received the first precipitation caused by cyclones. Surprisingly, we observed very weak diurnal signals in $\delta^{18}O_v$ and δD_v during either cyclone event (Figure 4), with amplitudes of diurnal variations in $\delta^{18}O_v$ (δD_v) of 1.10 ‰ (10.21 ‰) during cyclone Tauktae and 2.06 ‰ (16.07 ‰) during cyclone Yaas. The surface temperature and specific humidity showed an average peak-to-peak variability of about 7 °C and 2 g/kg, respectively, during the cyclone Tauktae. In contrast, these values were considerably lower during Yaas with respective peak-to-peak variabilities of about 3 °C and 0.94 g/kg. Unlike $\delta^{18}O_v$ and δD_v, d-excess$_v$ showed a clear diurnal pattern consisting of a gradual increase from early morning till about midday, followed by about 4:00 h during which d-excess remained at a high level, before starting to gradually decrease from about 16:00 h onward (Figure 4). This diurnal variation in d-excess$_v$ seems to have

https://doi.org/10.5194/egusphere-2023-2186
Preprint. Discussion started: 11 October 2023

been more prominent during cyclone Tauktae with a peak-to-peak variability of 3.87 ‰ (vs 1.90 ‰ during cyclone Yaas). The d-excess$_v$ diurnal cycle during Tauktae was strongly synchronized with surface temperature and specific humidity with respective correlation coefficients (R^2) of 0.96 and 0.81. During Yaas, the synchronicity was considerably weaker exhibiting correlation coefficients (R^2) of 0.27 and 0.35 with temperature and specific humidity, respectively. Considering that rather smaller precipitation amount during Tauktae compared to Yaas, neither $\delta^{18}O_v$ nor δD_v showed any notable diurnal signal during these events, indicating that any diurnal variation in $\delta^{18}O_v$ or δD_v during the cyclones events was independent of the day-night variation in local weather parameters and the Rayleigh fractionation processes they underwent during their northward movement (see Sect. 3.3 for a more detailed discussion); whereas local weather parameters may play pronounced roles on d-excess$_v$ diurnal variations depending on rainfall strength.

https://doi.org/10.5194/egusphere-2023-2186
Preprint. Discussion started: 11 October 2023

341 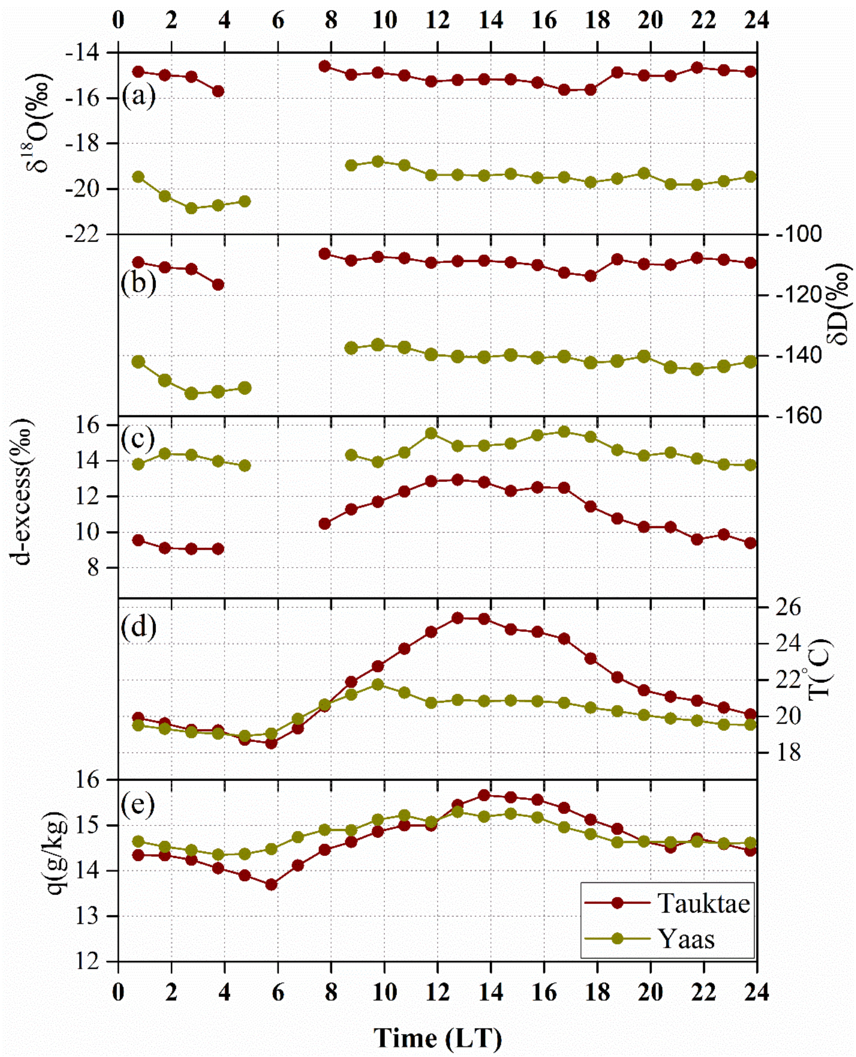

342 **Figure 4 Diurnal cycles of (a) $\delta^{18}O_v$, (b) δD_v, (c) d-excess$_v$, (d) temperature (T), and (e)**
343 **specific humidity (q) averaged from 19 to 22 May during Tauktae and from 25 to 28 May**
344 **during Yaas. The units of Time "LT" indicates Local Time.**

345

https://doi.org/10.5194/egusphere-2023-2186
Preprint. Discussion started: 11 October 2023

3.3 Isotopic response to regional climate

We now probe the underlying reasons for these isotopic variations in more detail. For this purpose, we analysed the influence of moisture sources on the isotopic composition of atmospheric water vapour by calculating 5-day backward trajectories for each day before, during, and after the cyclone events. We also calculated the associated specific humidity along the cyclone trajectories to estimate moisture uptake and identify possible rainfall regions (Figure 5).

Before the cyclone events, the majority of moisture trajectories associated with high $\delta^{18}O_v$ and δD_v originated either locally or were brought in by westerlies with low specific humidity along their paths. During Tauktae, most trajectories originate in the AS. During Yaas, most trajectories point to the BoB as the sole vapour source contributing to the moisture at the sampling site (Figure 5).

Both cyclone events have in common that the specific humidity tends to be high while they are over oceans and the air becomes drier while crossing over land, as moisture is removed through precipitation. We found that the association between both $\delta^{18}O_v$ and δD_v and Temperature/Relative humidity was much stronger during the cyclone events compared to before or after the events (Table 2). This might be linked to the cyclones transporting large amounts of moisture from remote oceans (Chen et al., 2021; Xu et al., 2019). After the cyclones had dissipated, the isotopic composition of atmospheric water vapour reverted to the original (enriched) levels ($\delta^{18}O_v$ = -14.64 ‰, δD_v= -103.97 ‰, and d-excess$_v$= 13.20 ‰).

https://doi.org/10.5194/egusphere-2023-2186
Preprint. Discussion started: 11 October 2023

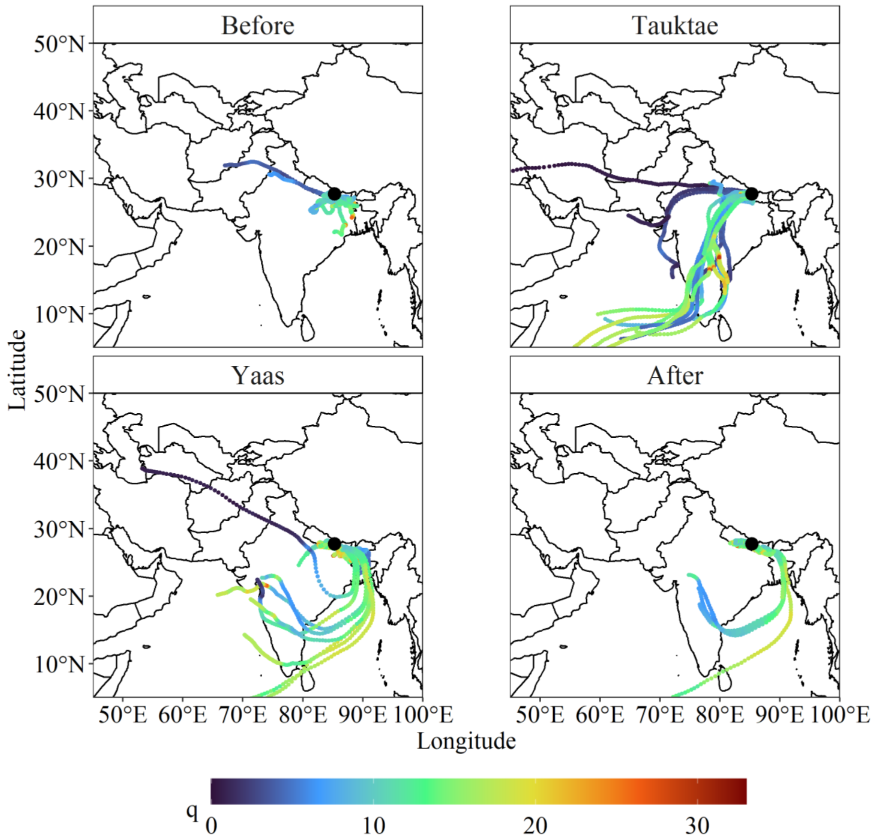

365

366 **Figure 5 Five-day backward moisture trajectories reaching the sampling site before,**
367 **during, and after the cyclone events. Colours denote specific humidity (q in g/kg) along the**
368 **trajectories.**

369 One of the most likely causes for large isotopic depletion during cyclone events might be
370 the associated convection processes. Several studies have demonstrated that convective
371 processes within tropical cyclones can cause the unusually depleted isotopic composition of
372 precipitation and atmospheric water vapour (Fudeyasu et al., 2008; Jackisch et al., 2022;
373 Munksgaard et al., 2015) due to a combination of strong cyclonic circulation, intense large-scale
374 convection, heavy precipitation, and high wind speeds (Chen et al., 2021; Xu et al., 2019). Here

https://doi.org/10.5194/egusphere-2023-2186
Preprint. Discussion started: 11 October 2023

we analyse the relationship between the isotopic composition of atmospheric water vapour and convective processes during two cyclone events, using outgoing longwave radiation (OLR) and vertical velocity as a proxy for convection. Due to the frequent co-occurrence of intense convection and significant mid-tropospheric convergence of moist air, the vertical velocities can also serve as a proxy for convective activity (Lekshmy et al., 2014). Fig. S5 and Fig. S6 depict the prevalence of strong convective processes associated with both cyclones throughout their entire lifespans. During the initial days of cyclone formation, OLR exceeded 260 Wm^{-2} in the area of the sampling site (Figs. S5 and S6) and had rather decreased rapidly to below 200 Wm^{-2} in the final stages of both cyclones when they were approaching the sampling site. Although the amount of precipitation associated with Tauktae (9.2 mm) was much lower than with Yaas (59.6 mm), $\delta^{18}O_v$ depleted by up to 12 ‰ during both cyclone events. Importantly, during both cyclones events, the progressive rainout was evident along the entire cyclone track, and the spatial distribution of precipitation was highly correlated with the convective process (as indicated by low OLR) (Figs. S7 and S8), suggesting that rainfall occurred from the deep convective cloud rather than from local evaporation. This interpretation was confirmed by comparing the regional precipitation to *in situ* measurements. According to Fig. S7 and Fig. S8, the measurement site received its first rainfall on 19 May during cyclone Tauktae and on 25 May during cyclone Yaas which we can confirm with our observation data. *In situ* observations show that during the days leading up to cyclone Tauktae, the sampling site received a total of 12.2 mm (from 7 May to 14 May) of precipitation with maximum rainfall of 9.2 mm/h recorded on 11 May at 13:00 h LT, which is equal to the total accumulated rainfall during the entire cyclone Tauktae. Although the pre-Tauktae and during-Tauktae rainfall amounts are similar, pre-cyclone $\delta^{18}O_v$ and δD_v were significantly more enriched (averages:$\delta^{18}O_v$ = -11.83 ‰ and δD_v = -80.30

https://doi.org/10.5194/egusphere-2023-2186
Preprint. Discussion started: 11 October 2023

‰) than during the cyclone event (averages: $\delta^{18}O_v$ = -13.59 ‰ and δD_v = -149.49 ‰). This confirms our previously stated hypothesis that the rainfall associated with cyclones causes significantly lower isotope values in vapour due to intense convective system (Gedzelman et al., 2003; Kurita, 2013), which is absent in localized rain events and on days without precipitation (Lekshmy et al., 2022).

Our hypothesis that isotopic variations during cyclone events at Kathmandu are mainly driven by convective processes is further supported by the Hovmöller diagram of OLR averaged over 80-90° E (Figure 6), which clearly shows that $\delta^{18}O_v$ depletion coincides with the presence of clouds. In contrast, d-excess$_v$ showed rather dissimilar variations between both cyclone events. Before the arrival of cyclone Tauktae, the daily averaged d-excess was above the global average of 10 ‰ (Fig. 6, horizontal orange line). Once Tauktae was approaching the sampling site, d-excess$_v$ decreased from around 12 ‰ to 10 ‰ and continued to oscillate about 10 ‰ until Tauktae had dissipated. As cyclone Yaas approached the measurement site with intense rainfall (Fig. 2), d-excess$_v$ ($\delta^{18}O_v$) gradually increased (decreased) while RH increased and air temperature decreased (Fig. 2). More specifically, d-excess$_v$ on 24 May was recorded as 12.82 ‰ when surface air temperature and surface RH was about 24 $^{\circ}$C and 70 % respectively. On 27 May, we noticed about a 3 ‰ rise in d-excess$_v$ when the surface temperature was reduced by 4°C and the surface RH was increased by 19 %. The combination of increasing d-excess and decreasing $\delta^{18}O_v$ has also been observed during the active convective phase of Madden-Julian oscillations (MJO) in the tropical atmosphere which highlights the role of vapour recycling due to the subsidence of air masses from stratiform clouds (Kurita et al., 2011). In addition, a large increase in d-excess$_v$ was also recorded in atmospheric vapour during cyclone Ita in 2014 and was attributed to downward moisture transport above the boundary layer (Munksgaard et al.,

https://doi.org/10.5194/egusphere-2023-2186
Preprint. Discussion started: 11 October 2023

2015). In our case, we did not find any statistically significant correlation during cyclone Yaas between d-excess$_v$ and RH/Temperature, although RH is generally considered an important parameter for interpreting d-excess values in atmospheric vapour and precipitation (Pfahl and Sodemann, 2014; Steen-Larsen et al., 2014). The observed co-occurrence of higher d-excess$_v$, lower temperatures, and high relative humidity (Fig. 2) points to kinetic fractionation processes either at a larger scale or in association with downdrafts (Conroy et al., 2016). This relationship also highlights the role played by the convective process with regard to the isotopic composition of atmospheric water vapour. Low $\delta^{18}O_v$ in combination with high d-excess$_v$ are known to be associated with rain re-evaporation under conditions of high saturation deficit because the addition of re-evaporated vapour to the atmosphere during precipitation events produces depleted cloud vapour and high d-excess (Conroy et al., 2016; Lekshmy et al., 2014). On normal days (without cyclones), high d-excess$_v$ values were generally accompanied by low RH (Figure 7) and vice versa. However, high relative humidities of the surface air together with near saturation conditions vertically (Figure 8, middle panel) during cyclone Yaas, rule out any effect of re-evaporation on increased (decreased) d-excess$_v$ ($\delta^{18}O_v$ and δD_v) values. Hence, we surmise that the higher d-excess$_v$ values during cyclone Yaas might be associated with downdrafts during convective rain events, which can transport isotopically depleted vapour with higher d-excess$_v$ values from the boundary layer to the surface (Kurita, 2013; Midhun et al., 2013).

https://doi.org/10.5194/egusphere-2023-2186
Preprint. Discussion started: 11 October 2023

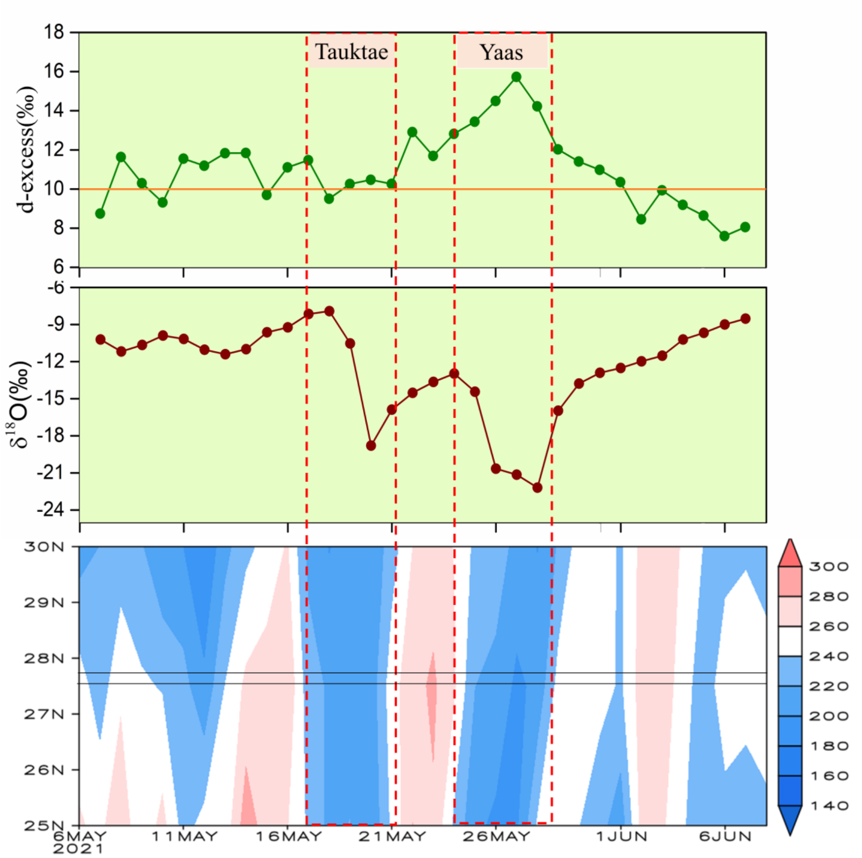

Figure 6 Time series of daily averaged d-excess$_v$ (top panel), $\delta^{18}O_v$ (middle panel), and Hovmöller diagram of NOAA interpolated OLR (W/m^2) averaged over 80° E-90° E (bottom panel) The orange horizontal line in the top panel represents the global average d-excess value (i.e. 10 ‰) and solid parallel lines in bottom panel depict the latitude range of sampling site.

https://doi.org/10.5194/egusphere-2023-2186
Preprint. Discussion started: 11 October 2023

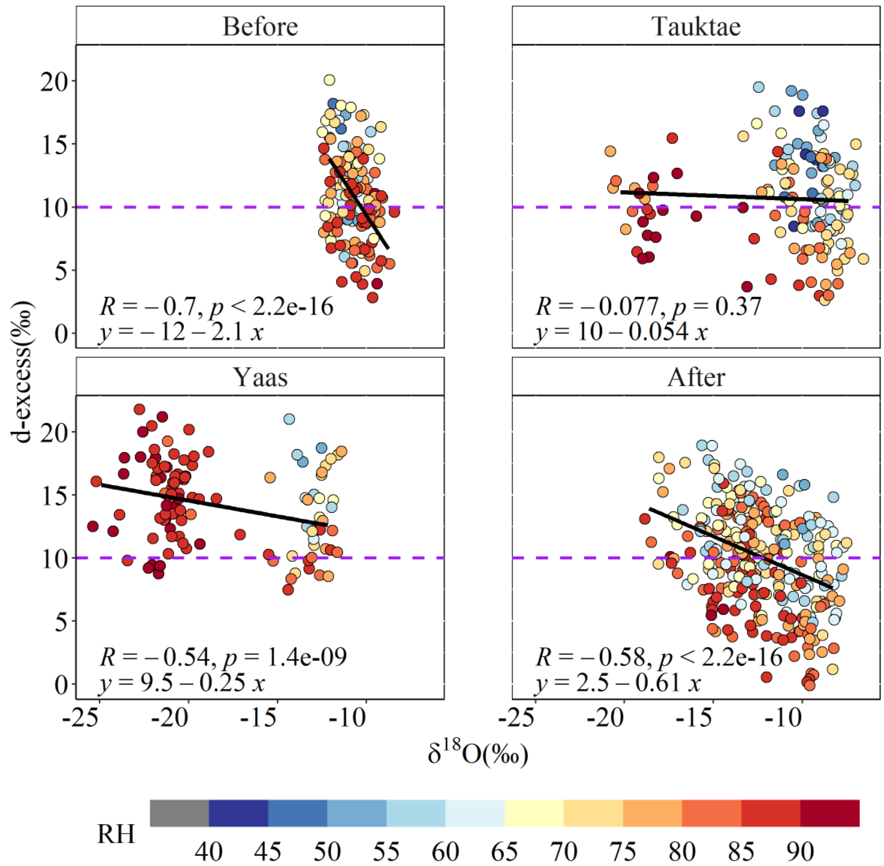

Figure 7 Scatter plots of d-excess$_v$ vs. $\delta^{18}O_v$ before, during, and after the cyclone events. The colour represents RH (in %) and the horizontal dashed purple lines represent the global average d-excess value (10 ‰).

To further elucidate the impact of convection on the isotopic composition of atmospheric water vapour, we analyzed the vertical distribution of vertical velocity, relative humidity, and air temperature averaged over a box between 25° N-28° N and 83° E-87° E which has our measurement site near its centre (Fig. 8). Our results show that strong shifts in $\delta^{18}O_v$, δD_v, and d-excess$_v$ during the cyclone events were strongly associated with vertical air motions (Figure 8).

https://doi.org/10.5194/egusphere-2023-2186
Preprint. Discussion started: 11 October 2023

We observed a general downward movement of air before the commencement of rainfall by Tauktae (i.e., from 7 May to around 18 May). The high depletion of $\delta^{18}O_v$ and δD_v during the final stages of Tauktae (Figure 2) was accompanied by strong upward air movement extending from 800 hPa to about 200 hPa (Figure 8). This upward motion was even stronger during cyclone Yaas and already became evident near the measurement site once Yaas made landfall at the BoB coast on 26 May. Interestingly, variations in RH at different pressure levels strongly coincided with changes in vertical velocity while the lower troposphere remained near saturation (RH= ~100 %) during the late stages of both cyclones. While the vertical air temperature showed the expected progressive decline with altitude, there were no significant temporal variations in temperature during the entire period, despite the high variation in RH. This implies that the high RH in the lower troposphere during both cyclone events was independent of temperature and hence the result of deep convection and the widespread development of clouds. The strong convective updraft added additional moisture from the warm ocean below, before passing over our measurement site (Lekshmy et al., 2014). Convective updrafts cause moisture to condense quickly and this high-efficiency condensation of heavy rain can result in more depleted $\delta^{18}O_v$ and δD_v (Lawrence and Gedzelman, 1996). In addition, we found a strong positive correlation between $\delta^{18}O_v$ and average vertical velocity (r=0.57) during Yaas at pressure levels between 300 hPa and 600 hPa in the area surrounding our study site (cf., Lekhsmy et al., 2014); During Tauktae, this correlation was weaker but still significant (r=0.30) (Fig. S9). This result suggests that the higher depletion in $\delta^{18}O_v$ and δD_v during cyclone Yaas relative to Tauktae may be due to the stronger convection associated with the BoB vapour compared to the AS vapour. The BoB is a convectively active region, and previous studies reported greater depletions in $\delta^{18}O_v$ and δD_v in precipitations with moisture from the BoB compared to the AS, irrespective of the season

https://doi.org/10.5194/egusphere-2023-2186
Preprint. Discussion started: 11 October 2023

(Breitenbach et al., 2010; Lekshmy et al., 2015; Midhun et al., 2018). Another reason why we observed different levels of isotope depletion between both cyclones may be related to differences in their closest proximity to the sampling site. While Yaas came as close as 400 km to our study site, Tauktae was still 1100 km away when it dissipated (Fig. S10). The closer proximity of Yaas may explain the stronger rainfall during that event which enhanced the isotopic fractionation which in turn led to stronger isotopic depletion (Jackisch et al., 2022). Similar results during the cyclone events have already been documented for precipitation stable isotopes (e.g., Fudeyasu et al., 2008; Jackisch et al., 2022; Munksgaard et al., 2015; Xu et al., 2019) and water vapour stable isotopes (e.g., Munksgaard et al., 2015; Rahul et al., 2016; Saranya et al., 2018). Even after both cyclones had dissipated, progressive rainfall continued at our sampling site due to the presence of residual moisture from the cyclones. Once these residual effects had diminished and rainfall intensity weakened, did both $\delta^{18}O_v$ and δD_v start to increase again (Fig. 2), likely due to evaporative effects (Munksgaard et al., 2015; Xu et al., 2019; Jackisch et al., 2022).

https://doi.org/10.5194/egusphere-2023-2186
Preprint. Discussion started: 11 October 2023

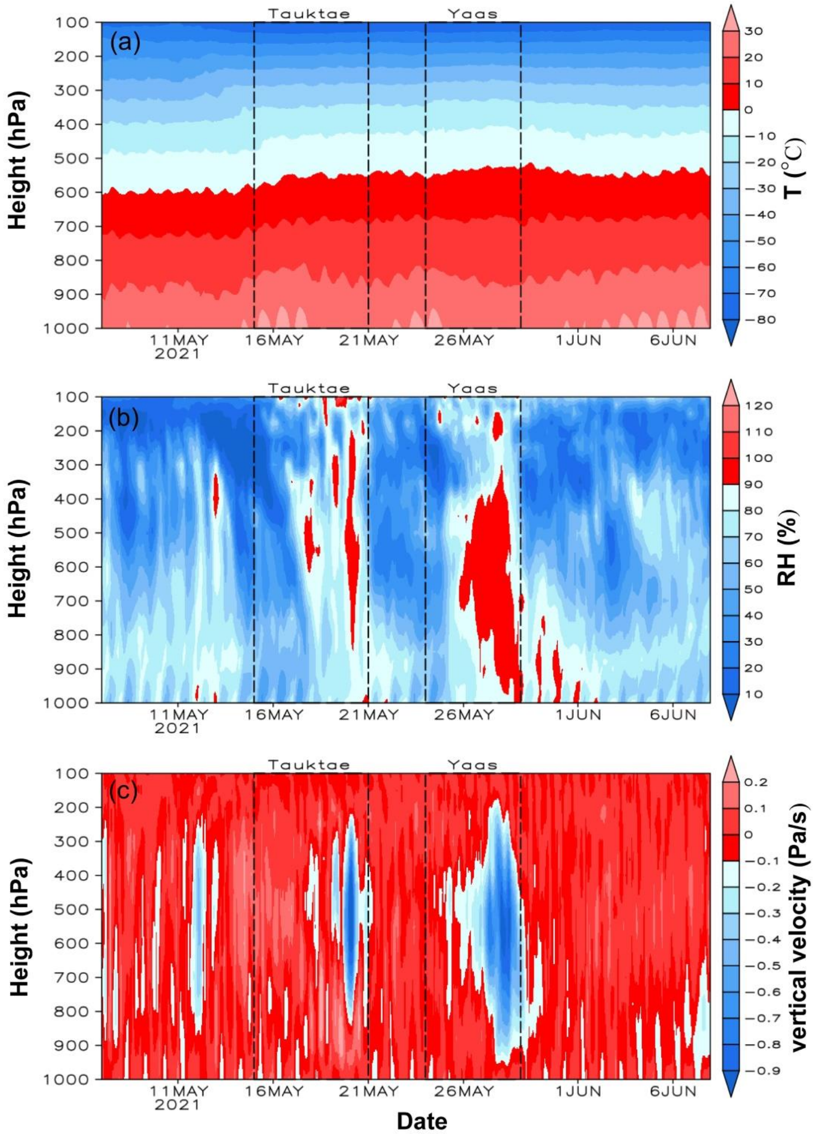

Figure 8 Time series of the vertical distribution of air temperature (top), RH (middle), and vertical velocity (bottom) averaged over 25° N-28° N and 83° E-87° E with Kathmandu approximately at the centre. Negative (positive) vertical velocities indicate ascending (descending) winds.

https://doi.org/10.5194/egusphere-2023-2186
Preprint. Discussion started: 11 October 2023

Examining a plot of δD_v vs specific humidity, combined with the Rayleigh distillation and mixing curves, we can assess the mixing conditions during the study period (Figure 9). Before the development of cyclone Tauktae and during its early stages, the data points lie well above the mixing curve, suggesting a significant contribution of vapour from local evapotranspiration. In contrast, during the later stages of Tauktae, δD_v was significantly depleted to levels well below the Rayleigh curve. Similarly, during the early stage of cyclone Yaas, there are only a few data points between the mixing and Rayleigh curves with the majority well below the Rayleigh curve, particularly during the late stage of Yaas. These results indicate the influences of mixing processes and re-evaporation below clouds as described previously (Galewsky and Samuels-Crow, 2015). After Yaas had dissipated, δD_v gradually increased again with about half of the data points clustered between the mixing and Rayleigh curves and the remaining data points well above the mixing curve, indicating a strong influence of mixing processes and locally evaporated vapour, which is also evidenced by the moisture backward trajectories (Figure 5 lower right panel).

https://doi.org/10.5194/egusphere-2023-2186
Preprint. Discussion started: 11 October 2023

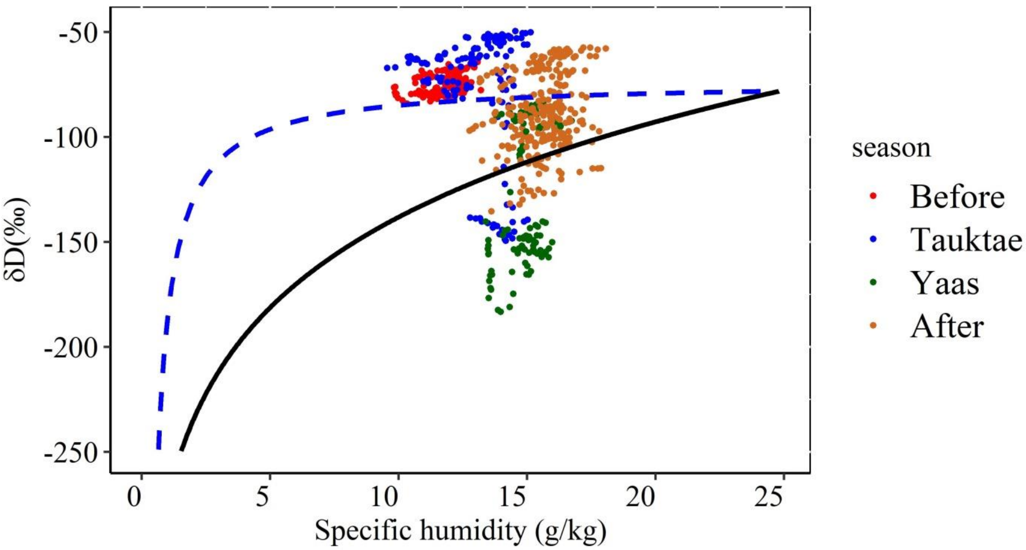

Figure 9 Scatter plot of hourly averaged δD_v vs. specific humidity (q). The solid black curve represents the Rayleigh distillation curve calculated for the initial condition of δD_v =- 78.20 ‰, BoB-averaged δD_v (Lekshmy et al., 2022), SST of 30° C, and RH of 90 %. The dashed blue curve represents the mixing line, calculated based on dry continental air (q= 0.5 g/kg and δD_v =-300 ‰ (Wang et al., 2021)) and the wet source, which corresponds to the initial conditions used to calculate the theoretical Rayleigh curve.

3.4 Relationships between local weather parameters and vapour $\delta^{18}O$, δD, and d-excess

Besides regional influences, we also analyzed whether changes in local meteorological conditions impact the variations in the isotopic composition of atmospheric water vapour. Before the cyclone events, both $\delta^{18}O_v$ and δD_v showed significant negative correlations with local air temperature and wind speed and significant positive correlations with relative humidity (Table 2). This correlation between $\delta^{18}O_v/\delta D_v$ and relative humidity became negative during the

https://doi.org/10.5194/egusphere-2023-2186
Preprint. Discussion started: 11 October 2023

two cyclone events, with a significant temperature effect also present. We hypothesize that the progressive rainout during the cyclone events followed a temperature decrease (Figure 2), which would result in this $\delta^{18}O_v/\delta D_v$ correlation with temperature (Delattre et al., 2015). However, the strength of the correlations between $\delta^{18}O_v/\delta D_v$ and local meteorological parameters varied significantly throughout the lifetimes of both cyclones. For instance, the effects of temperature and relative humidity on $\delta^{18}O_v$ were stronger (r=0.68 for temperature and r=-0.74 for RH) during Yaas compared to Tauktae (r=0.34 for temperature and r=-0.49 for relative humidity). The weaker relationship during Tauktae is likely due to the significantly lower rainfall amounts relative to Yaas. The cooling of surface air during rainfall and the associated isotopic equilibrium of vapour with raindrops cause a positive correlation between $\delta^{18}O_v/\delta D_v$ and temperature (Midhun et al., 2013). This process was more favourable during Yaas with its stronger and more continuous rainfall (Fig. 2). During Tauktae, we did not observe any effect of precipitation amount on the isotopic composition of atmospheric water vapour, while during Yaas there was a strong negative correlation (r=-0.56) between them. Recent studies have suggested that the impact of rainfall amount is not a purely local phenomenon (Galewsky et al., 2016) but modulated by convective and large-scale properties such as downdraft moisture recycling (Risi et al., 2008), large-scale organized convection and associated stratiform rain (Kurita, 2013), and regional circulation and shifting moisture source regions (Lawrence et al., 2004). During cyclone Yaas, our measurements showed the presence of an intense convective system over our study site which indicates that the observed rainfall amount effect may have been controlled by moisture convergence (Chakraborty et al., 2016). Subsequent rainfall from the convective system over a region with depleted isotope values resulted in a negative association between precipitation amount and $\delta^{18}O_v/\delta D_v$ (Kurita, 2013). Furthermore, the negative correlation between $\delta^{18}O_v/\delta D_v$

https://doi.org/10.5194/egusphere-2023-2186
Preprint. Discussion started: 11 October 2023

and RH together with the fact that $\delta^{18}O_v/\delta D_v$ was depleted during both cyclone events highlight the influence of humid moisture sources on the isotopic composition of atmospheric water vapour (Yu et al., 2008), which was also confirmed by our moisture backward trajectory analysis (Fig. 5). A strong negative correlation between δD_v and RH was also observed in mid-tropospheric water vapour over the western Pacific associated with intense convective activity (Noone, 2012). It is noteworthy that the relationship between $\delta^{18}O_v/\delta D_v$ and temperature before and after the cyclone events degraded significantly, which might be due to the admixture of vapour originating from plant transpiration during that period (Delattre et al., 2015).

As discussed above, $\delta^{18}O_v$ and δD_v were strongly associated with air temperature and RH during cyclone Yaas but less so during cyclone Tauktae. In contrast, d-excess$_v$ was positively (negatively) correlated with local air temperature (local RH) before, during Tauktae, and after both cyclone events, whilst no significant correlations were seen during cyclone Yaas (Table 2). This indicates that local moisture recycling may have played a crucial role at our sampling site, while the absence of any correlation of d-excess$_v$ with RH during Yaas implies that RH might not be a reliable predictor of kinetic fractionation during evaporation at our site. In addition, while about 75% of RH measurements during Yaas yielded high values (i.e., RH >80%), this fraction was only 25% during Tauktae. Previous studies (e.g., Midhun et al., 2013; Uemura et al., 2008) highlighted that the relation between d-excess$_v$ and RH weakens above RH=80%, which may explain the weaker relation of d-excess$_v$ and RH during Yaas.

https://doi.org/10.5194/egusphere-2023-2186
Preprint. Discussion started: 11 October 2023

Table 2 Linear correlations between the isotopic composition of atmospheric water vapor ($\delta^{18}O_v$, δD_v, and d-excess$_v$) and air temperature (T), relative humidity (RH), precipitation amount (P), wind speed (WS), and dew point temperature (T_d) before, during, and after the cyclone events. *,**, and * indicate correlation significance levels of 0.001, 0.01, and 0.05 respectively.**

	T	RH	P	WS	T_d
			Before		
$\delta^{18}O_v$	-0.34^{***}	0.45^{***}	-0.41	-0.45^{***}	0.16
δD_v	-0.1	0.28^{***}	-0.37	-0.28^{***}	0.41^{***}
d-excess$_v$	0.68^{***}	-0.61^{***}	0.35	0.59^{***}	0.40^{***}
			Cyclone Tauktae		
$\delta^{18}O_v$	0.34^{***}	-0.49^{***}	0.11	0.20^{*}	-0.22^{**}
δD_v	0.41^{***}	-0.55^{***}	0.10	0.26^{**}	-0.20^{**}
d-excess$_v$	0.79^{***}	-0.67^{***}	-0.22	0.75^{***}	0.19^{*}
			Cyclone Yaas		
$\delta^{18}O_v$	0.68^{***}	-0.74^{***}	-0.56^{***}	0.05	0.28^{**}
δD_v	0.70^{***}	-0.76^{***}	-0.56^{***}	0.06	0.30^{**}
d-excess$_v$	-0.003	0.1	0.19	0.27^{**}	0.19^{*}
			After		
$\delta^{18}O_v$	0.13^{*}	-0.13^{*}	-	0.14^{*}	0.10
δD_v	0.22^{***}	-0.22^{***}	-	0.21^{***}	0.18^{**}
d-excess$_v$	0.56^{***}	-0.54^{***}	-	0.47^{***}	0.47^{***}

4 Conclusion

This study presented the results of continuous measurements of the isotopic composition of atmospheric water vapour over Kathmandu between 7 May and 7 June 2021 covering two cyclone events, namely cyclone Tauktae formed over the Arabian Sea, and cyclone Yaas formed over the Bay of Bengal. Both cyclone events led to significant depletion of $\delta^{18}O_v$ and δD_v, with $\delta^{18}O_v$ decreasing by over 12 ‰ between May 14 and May 20 (during Tauktae) as well as between May 24 and May 29 (during Yaas). We could attribute those rapid depletions to changes in moisture sources (local vs. marine) that were inferred from backward moisture trajectories.

https://doi.org/10.5194/egusphere-2023-2186
Preprint. Discussion started: 11 October 2023

Similar slopes and intercepts of meteoric vapour line with GMWL during both cyclone events indicate the occurrence of surface recharge following convective conditions. The lower intercepts before and after the cyclone events highlight the influence of non-equilibrium processes such as evaporation on the isotopic composition of atmospheric water vapour.

Despite significant diurnal fluctuations in temperature and specific humidity during both cyclone events, $\delta^{18}O_v$ and δD_v exhibit weak diurnal signals which rule out any impact of day-night variations in local weather parameters. Instead, these discrepancies might reflect different cyclone sources and convection processes they underwent along their northward trajectories. The OLR and regional precipitation during cyclone events together with the observed correlation between vertical velocity and $\delta^{18}O_v$ showed high moisture convergence and heavy convection at and around the measurement site which caused unusually depleted $\delta^{18}O_v$ during that period. Moisture convergence and convection were stronger during cyclone Yaas which resulted in higher (lower) d-excess$_v$ ($\delta^{18}O_v$) values during Yaas, compared to Tauktae, possibly due to strong downdrafts during the cyclone-related convective rain events which can transport vapour with higher (lower) d-excess$_v$ ($\delta^{18}O_v$) values toward the surface. During the cyclone events, and in contrast to immediately before and after these events, there was a strong linear association between the isotopic compositions of atmospheric water vapour and local meteorological parameters, which led us to conclude that the progressive rainout during the cyclone events followed a temperature decrease and RH increase, which would, in turn, produce a $\delta^{18}O_v/\delta D_v$ correlation with temperature and RH. This type of association may visible in the cyclones' moisture characteristics as each cyclone transported high RH from a remote ocean inland, which suggested that their specific water vapour stable isotopic signatures could still be observed as far north as Kathmandu.

https://doi.org/10.5194/egusphere-2023-2186
Preprint. Discussion started: 11 October 2023

Overall, our results showed that tropical cyclones that originated in the BoB and AS during the pre-monsoon season transported large amounts of isotopically depleted vapour and produced moderate to heavy rainfall over a sizeable region in Nepal. Hence the isotopic composition of atmospheric water vapour and precipitation during the dry season should be interpreted with caution and the effects of cyclones should not be underestimated. Additionally, our results further underline the need for simultaneous measurements of the isotopic composition of both atmospheric water vapour and precipitation to better understand post-condensation exchanges between falling raindrops and boundary layer vapour over Kathmandu.

https://doi.org/10.5194/egusphere-2023-2186
Preprint. Discussion started: 11 October 2023

Data Availability

Data will be available upon request from the corresponding author.

Competing interests

The contact author has declared that none of the authors has any competing interests.

Acknowledgements

This work was funded by 'The Second Tibetan Plateau Scientific Expedition' (Grant No. 2019QZKK0208) and the National Natural Science Foundation of China (Grants 41922002 and 41988101-03). We thank Yulong Yang for his assistance with instrument set-up and initial running.

Author contributions

Niranjan Adhikari: Data curation, Formal analysis, Writing - Original draft preparation. **Jing Gao**: Data curation, Conceptualization, Methodology, Supervision, Writing - Review and Editing, Funding acquisition. **Aibin Zhao**: measuring assistance, Writing – Editing. **Tianli Xu**, **Manli Chen,** and **Xiaowei Niu**: measuring assistance. **Tandong Yao**: Supervision, Funding acquisition.

https://doi.org/10.5194/egusphere-2023-2186
Preprint. Discussion started: 11 October 2023

References

Acharya, S., Yang, X., Yao, T., Shrestha, D.: Stable isotopes of precipitation in Nepal Himalaya highlight the topographic influence on moisture transport, Quat. Int., 565, 22–30, https://doi.org/10.1016/j.quaint.2020.09.052, 2020.

Adhikari, N., Gao, J., Yao, T., Yang, Y., Dai, D.: The main controls of the precipitation stable isotopes at Kathmandu, Nepal, Tellus, Ser. B Chem. Phys. Meteorol., 72, 1–17. https://doi.org/10.1080/16000889.2020.1721967, 2020

Bohlinger, P., Sorteberg, A., Sodemann, H.: Synoptic conditions and moisture sources actuating extreme precipitation in Nepal, J. Geophys. Res. Atmos., 122, 12–653, https://doi.org/10.1002/2017JD027543, 2017.

Boschi, R., Lucarini, V.: Water pathways for the Hindu-Kush-Himalaya and an analysis of three flood events, Atmosphere, 10, 489, https://doi.org/10.3390/atmos10090489, 2019.

Brand, W.A., Geilmann, H., Crosson, E.R., Rella, C.W.: Cavity ring-down spectroscopy versus high-temperature conversion isotope ratio mass spectrometry; a case study on delta (2) H and delta (18) O of pure water samples and alcohol/water mixtures, Rapid Commun. mass Spectrom, RCM 23, 1879–1884, https://doi.org/10.1002/rcm.4083, 2009.

Breitenbach, S.F.M., Adkins, J.F., Meyer, H., Marwan, N., Kumar, K.K., Haug, G.H.: Strong influence of water vapor source dynamics on stable isotopes in precipitation observed in Southern Meghalaya, NE India, Earth Planet. Sci. Lett., 292, 212–220, https://doi.org/10.1016/j.epsl.2010.01.038, 2010.

Chakraborty, S., Sinha, N., Chattopadhyay, R., Sengupta, S., Mohan, P.M., Datye, A., 2016.

https://doi.org/10.5194/egusphere-2023-2186
Preprint. Discussion started: 11 October 2023

Atmospheric controls on the precipitation isotopes over the Andaman Islands, Bay of Bengal, Sci. Rep., 6, 1–11, https://doi.org/10.1038/srep19555, 2016.

Chan, K.T.F., Chan, J.C.L., Zhang, K., Wu, Y.: Uncertainties in tropical cyclone landfall decay, npj Clim. Atmos. Sci., 5, 93, https://doi.org/10.1038/s41612-022-00320-z, 2022.

Chen, F., Huang, C., Lao, Q., Zhang, S., Chen, C., Zhou, X., Lu, X., Zhu, Q.: Typhoon Control of Precipitation Dual Isotopes in Southern China and Its Palaeoenvironmental Implications, J. Geophys. Res. Atmos., 126, 1–15, https://doi.org/10.1029/2020JD034336, 2021.

Chhetri, T.B., Yao, T., Yu, W., Ding, L., Joswiak, D., Tian, L., Devkota, L.P., Qu, D.: Stable isotopic compositions of precipitation events from Kathmandu, southern slope of the Himalayas, Chinese Sci. Bull., 59, 4838–4846, https://doi.org/10.1007/s11434-014-0547-4, 2014.

Conroy, J.L., Noone, D., Cobb, K.M., Moerman, J.W., Konecky, B.L.: Paired stable isotopologues in precipitation and vapor: A case study of the amount effect within western tropical Pacific storms, J. Geophys. Res. Atmos., 121, 3290–3303, https://doi.org/10.1002/2015JD023844, 2016.

Dansgaard, W.: Stable isotopes in precipitation, Tellus 16, 436–468, https://doi.org/10.3402/tellusa.v16i4.8993, 1964

Delattre, H., Vallet-Coulomb, C., Sonzogni, C.: Deuterium excess in the atmospheric water vapour of a Mediterranean coastal wetland: Regional vs. local signatures, Atmos. Chem. Phys., 15, 10167–10181, https://doi.org/10.5194/acp-15-10167-2015, 2015

Draxler, R.R., Hess, G.D.: Description of the HYSPLIT4 modeling system, 1997.

https://doi.org/10.5194/egusphere-2023-2186
Preprint. Discussion started: 11 October 2023

Fudeyasu, H., Ichiyanagi, K., Sugimoto, A., Yoshimura, K., Ueta, A., Yamanaka, M.D., Ozawa, K.: Isotope ratios of precipitation and water vapor observed in Typhoon Shanshan, J. Geophys. Res. Atmos, https://doi.org/10.1029/2007JD009313, 113, 2008.

Galewsky, J., Samuels-Crow, K.: Summertime moisture transport to the southern South American Altiplano: Constraints from in situ measurements of water vapor isotopic composition, J. Clim., 28, 2635–2649, https://doi.org/10.1175/JCLI-D-14-00511.1, 2015.

Galewsky, J., Steen-larsen, H.C., Field, R.D., Risi, W.C., Schneider, M.: Stable isotopes in athmospheric water vapor and application to the hydrologic cycle., Rev. Geophys. submitted, 1–169, https://doi.org/10.1002/2015RG000512, 2016.

Gaona, M.F.R., Villarini, G., Zhang, W., Vecchi, G.A.: The added value of IMERG in characterizing rainfall in tropical cyclones, Atmos. Res., doi:10.1016/j.atmosres.2018.03.008, 209, 95–102, 2018.

Gedzelman, S., Lawrence, J., Gamache, J., Black, M., Hindman, E., Black, R., Dunion, J., Willoughby, H., Zhang, X.: Probing hurricanes with stable isotopes of rain and water vapor, Mon. Weather Rev, https://doi.org/10.1175/1520-0493(2003)131<1112:phwsio>2.0.co;2, 131, 1112–1127, 2003.

Han, X., Lang, Y., Wang, T., Liu, C.Q., Li, F., Wang, F., Guo, Q., Li, S., Liu, M., Wang, Y., Xu, A.: Temporal and spatial variations in stable isotopic compositions of precipitation during the typhoon Lekima (2019), China. Sci. Total Environ., 762, https://doi.org/10.1016/j.scitotenv.2020.143143, 2021

Hoffmann, G., Cuntz, M., Jouzel, J., Werner, M.: A systematic comparison between the

IAEA/GNIP isotope network and the ECHAM 4 atmospheric general circulation model, Isot. Water Cycle Past, Present Futur. a Dev. Sci., 303–320, 2005.

Huffman, G.J., Bolvin, D., Braithwaite, D., Hsu, K., Joyce, R., Kidd, C., Nelkin, E.J., Sorooshian, S., Tan, J., Xie, P.: Algorithm Theoretical Basis Document (ATBD) of Integrated Multi-satellitE Retrievals for GPM (IMERG), version 4.6. Nasa 29, 2017.

Jackisch, D., Yeo, B.X., Switzer, A.D., He, S., Cantarero, D.L.M., Siringan, F.P., Goodkin, N.F.: Precipitation stable isotopic signatures of tropical cyclones in Metropolitan Manila, Philippines, show significant negative isotopic excursions, Nat. Hazards Earth Syst. Sci., 22, 213–226, https://doi.org/10.5194/nhess-22-213-2022, 2022.

Kendall, C., Caldwell, E.A.: Fundamentals of Isotope Geochemistry, Isot. Tracers Catchment Hydrol., 51–86, https://doi.org/10.1016/B978-0-444-81546-0.50009-4, 1998.

Kleist, D.T., Parrish, D.F., Derber, J.C., Treadon, R., Wu, W.-S., Lord, S.: Introduction of the GSI into the NCEP global data assimilation system, Weather Forecast., 24, 1691–1705, https://doi.org/10.1175/2009waf2222201.1, 2009.

Knapp, K.R., Kruk, M.C., Levinson, D.H., Diamond, H.J., Neumann, C.J.: The international best track archive for climate stewardship (IBTrACS) unifying tropical cyclone data, Bull. Am. Meteorol. Soc., 91, 363–376, https://doi.org/10.1175/2009bams2755.1, 2010.

Krishnamurthy, V., Shukla, J.: Intraseasonal and seasonally persisting patterns of Indian monsoon rainfall, J. Clim., 20, 3–20, https://doi.org/10.1175/jcli3981.1, 2007.

Kurita, N.: Water isotopic variability in response to mesoscale convective system over the tropical ocean, J. Geophys. Res. Atmos., 118, 10,376-10,390,

https://doi.org/10.5194/egusphere-2023-2186
Preprint. Discussion started: 11 October 2023

https://doi.org/10.1002/jgrd.50754, 2013.

Kurita, N., Noone, D., Risi, C., Schmidt, G.A., Yamada, H., Yoneyama, K.: Intraseasonal isotopic variation associated with the Madden-Julian Oscillation, J. Geophys. Res. Atmos., 116, 1–20, https://doi.org/10.1029/2010JD015209, 2011.

Lawrence, J.R., Gedzelman, S.D., Dexheimer, D., Cho, H.K., Carrie, G.D., Gasparini, R., Anderson, C.R., Bowman, K.P., Biggerstaff, M.I.: Stable isotopic composition of water vapor in the tropics, J. Geophys. Res. Atmos., 109 (D6), https://doi.org/10.1029/2003jd004046, 2004.

Lawrence, J.R., Gedzelman, S.D., Gamache, J., Black, M.: Stable isotope ratios: hurricane Olivia, J. Atmos. Chem., 41, 67–82, 2002.

Lawrence, J.R., Gedzelman, S.D., Zhang, X., Arnold, R.: Stable isotope ratios of rain and vapor in 1995 hurricanes, J. Geophys. Res. Atmos., 103, 11381–11400, https://doi.org/10.1029/97jd03627, 1998.

Lawrence, R.J., Gedzelman, D.S.: Low stable isotope ratios of tropical cyclone rains, Geophys. Res. Lett., 23, 527–530, https://doi.org/10.1029/96gl00425,1996.

Lekshmy, P.R., Midhun, M., Ramesh, R.: Role of moisture transport from Western Pacific region on water vapor isotopes over the Bay of Bengal, Atmos. Res., 265, 105895, https://doi.org/10.1016/j.atmosres.2021.105895, 2022.

Lekshmy, P.R., Midhun, M., Ramesh, R.: Spatial variation of amount effect over peninsular India and Sri Lanka: Role of seasonality, Geophys. Res. Lett., 42(13), 5500–5507, https://doi.org/10.1002/2015GL064517, 2015.

Lekshmy, P.R., Midhun, M., Ramesh, R., Jani, R.A.: ^{18}O depletion in monsoon rain relates to large scale organized convection rather than the amount of rainfall, Sci. Rep., 4, 1–5. https://doi.org/10.1038/srep05661, 2014.

Li, L., Chakraborty, P.: Slower decay of landfalling hurricanes in a warming world, Nature 587, 230–234, https://doi.org/10.1038/s41586-020-2867-7, 2020.

Li, Z., Yu, W., Li, T., Murty, V.S.N., Tangang, F.: Bimodal character of cyclone climatology in the Bay of Bengal modulated by monsoon seasonal cycle, J. Clim., 26 (3), 1033–1046, https://doi.org/10.1175/jcli-d-11-00627.1, 2013.

Liebmann, B., Smith, C.A.: Description of a complete (interpolated) outgoing longwave radiation dataset, Bull. Am. Meteorol. Soc., 77, 1275–1277, 1996.

Liu, Z., Tian, L., Yao, T., Yu, W.: Seasonal deuterium excess in Nagqu precipitation: Influence of moisture transport and recycling in the middle of Tibetan Plateau, Environ. Geol., 55, 1501–1506, https://doi.org/10.1007/s00254-007-1100-4, 2008.

Midhun, M., Lekshmy, P.R., Ramesh, R.: Hydrogen and oxygen isotopic compositions of water vapor over the Bay of Bengal during monsoon, Geophys. Res. Lett., 40, 6324–6328, https://doi.org/10.1002/2013GL058181, 2013.

Midhun, M., Pr, L., Ramesh, R., Yoshimura, K., Kk, S.: The effect of monsoon circulation on the stable isotopic composition of rainfall, J. Geophys. Res. Atmos., 123, 5205-5221, https://doi.org/10.1029/2017JD027427, 2018.

Mohapatra, M., Srivastava, A.K., Balachandran, S., Geetha, B.: Inter-annual variation and trends in Tropical Cyclones and Monsoon Depressions over the North Indian Ocean. Observed

Climate Variability and Change over the Indian Region, Springer Geology, 89–106, https://doi.org/ 10.1007/978-981-10-2531-0_6, 2016.

Munksgaard, N.C., Zwart, C., Kurita, N., Bass, A., Nott, J., Bird, M.I.: Stable isotope anatomy of tropical cyclone ita, North-Eastern Australia, April 2014, PLoS One 10, 1–15, https://doi.org/10.1371/journal.pone.0119728, 2015.

Noone, D.: Pairing measurements of the water vapor isotope ratio with humidity to deduce atmospheric moistening and dehydration in the tropical midtroposphere, J. Clim., 25, 4476–4494, https://doi.org/10.1175/JCLI-D-11-00582.1, 2012.

Pandya, U., Khandelval, S., Sanghvi, H., Joshi, E., Vekaria, G.L., Jaaffrey, S.N.A., Soni, M.: Cyclone 'TAUKTAE'-Observed through data & satellite images, 2021.

Paul, S., Chowdhury, S.: Investigation of the character and impact of tropical cyclone Yaas: a study over coastal districts of West Bengal, India, Saf. Extrem. Environ., 3, 219–235, https://doi.org/10.1007/s42797-021-00044-y, 2021.

Payne, V.H., Noone, D., Dudhia, A., Piccolo, C., Grainger, R.G.: Global satellite measurements of HDO and implications for understanding the transport of water vapour into the stratosphere, Q. J. R. Meteorol. Soc., 133, 1459–1471, https://doi.org/10.1002/qj, 2007.

Pfahl, S., Sodemann, H.: What controls deuterium excess in global precipitation? Clim. Past, 10, 771–781, https://doi.org/10.5194/cp-10-771-2014, 2014..

Rahul, P., Ghosh, P., Bhattacharya, S.K., Yoshimura, K.: Controlling factors of rainwater and water vapor isotopes at Bangalore, India: Constraints from observations in 2013 Indian monsoon, J. Geophys. Res., 121, 13,936-13,952, https://doi.org/10.1002/2016JD025352,

https://doi.org/10.5194/egusphere-2023-2186
Preprint. Discussion started: 11 October 2023

2016.

Rajeev, A., Mishra, V.: Observational evidence of increasing compound tropical cyclone-moist heat extremes in India, Earth's Futur., 10, e2022EF002992, https://doi.org/10.1029/2022ef002992, 2022.

Risi, C., Bony, S., Vimeux, F.: Influence of convective processes on the isotopic composition ($\delta^{18}O$ and δD) of precipitation and water vapor in the tropics: 2. Physical interpretation of the amount effect, J. Geophys. Res. Atmos., 113, 1–12, https://doi.org/10.1029/2008JD009943, 2008.

Sánchez-Murillo, R., Durán-Quesada, A.M., Esquivel-Hernández, G., Rojas-Cantillano, D., Birkel, C., Welsh, K., Sánchez-Llull, M., Alonso-Hernández, C.M., Tetzlaff, D., Soulsby, C., Boll, J., Kurita, N., Cobb, K.M.: Deciphering key processes controlling rainfall isotopic variability during extreme tropical cyclones, Nat. Commun., 10, 1–10, https://doi.org/10.1038/s41467-019-12062-3, 2019.

Saranya, P., Krishan, G., Rao, M.S., Kumar, S., Kumar, B.: Controls on water vapor isotopes over Roorkee, India: Impact of convective activities and depression systems, J. Hydrol., 557, 679–687, https://doi.org/10.1016/j.jhydrol.2017.12.061, 2017.

Steen-Larsen, H.C., Sveinbjörnsdottir, A.E., Peters, A.J., Masson-Delmotte, V., Guishard, M.P., Hsiao, G., Jouzel, J., Noone, D., Warren, J.K., White, J.W.C.: Climatic controls on water vapor deuterium excess in the marine boundary layer of the North Atlantic based on 500 days of in situ, continuous measurements, Atmos. Chem. Phys., 14, 7741–7756, https://doi.org/10.5194/acp-14-7741-2014, 2014.

https://doi.org/10.5194/egusphere-2023-2186
Preprint. Discussion started: 11 October 2023

Sun, C., Tian, L., Shanahan, T.M., Partin, J.W., Gao, Y., Piatrunia, N., Banner, J.: Isotopic variability in tropical cyclone precipitation is controlled by Rayleigh distillation and cloud microphysics, Commun. Earth Environ., 3, https://doi.org/10.1038/s43247-022-00381-1, 2022.

Tian, L., Yao, T., Numaguti, A., Sun, W.: Stable isotope variations in monsoon precipitation on the Tibetan Plateau, J. Meteorol. Soc. Japan., 79, 959–966, https://doi.org/10.2151/jmsj.79.959, 2001.

Uemura, R., Matsui, Y., Yoshimura, K., Motoyama, H., Yoshida, N.: Evidence of deuterium excess in water vapor as an indicator of ocean surface conditions, J. Geophys. Res. Atmos., 113, https://doi.org/10.1029/2008jd010209, 2008.

Verma, K., Gupta, A., 2021. Cyclone Tauktae: Cyclones, Their Impacts and Disasters Risk Management.

Villarini, G., Smith, J.A., Baeck, M.L., Marchok, T., Vecchi, G.A.: Characterization of rainfall distribution and flooding associated with US landfalling tropical cyclones: Analyses of Hurricanes Frances, Ivan, and Jeanne (2004), J. Geophys. Res. Atmos., 116, https://doi.org /10.1029/2011jd016175, 2011.

Worden, J., Noone, D., Bowman, K.: Importance of rain evaporation and continental convection in the tropical water cycle, Nature, 445, 528–532, https://doi.org /10.1038/nature05508, 2007.

Xu, T., Sun, X., Hong, H., Wang, X., Cui, M., Lei, G., Gao, L., Liu, J., Lone, M.A., Jiang, X.: Stable isotope ratios of typhoon rains in Fuzhou, Southeast China, during 2013–2017. J.

https://doi.org/10.5194/egusphere-2023-2186
Preprint. Discussion started: 11 October 2023

Hydrol., 570, 445–453, https://doi.org/10.1016/j.jhydrol.2019.01.017, 2019.

Yoshimura, K.: Stable Water Isotopes in Climatology, Meteorology, and Hydrology: A Review, J. Meteorol. Soc. Japan, 93, 513–533, https://doi.org/10.2151/jmsj.2015-036, 2015.

Yu, W., Yao, T., Tian, L., Ma, Y., Ichiyanagi, K., Wang, Y., Sun, W.: Relationships between $\delta^{18}O$ in precipitation and air temperature and moisture origin on a south-north transect of the Tibetan Plateau, Atmos. Res., 87, 158–169, https://doi.org/10.1016/j.atmosres.2007.08.004, 2008.